REPORTS OF PRACTICAL ONCOLOGY AND RADIOTHERAPY 24 (2019) 576–584

Available online at www.sciencedirect.com

ScienceDirect

journal homepage: http://www.elsevier.com/locate/rpor

Original research article

Dose distribution comparison in volumetric-modulated arc therapy plans for head and neck cancers with and without an external body contour extended technique

Yoshihiro Tanaka[a], *Hajime Monzen*[b,*], *Kenji Matsumoto*[c], *Shinichiro Inomata*[a], *Toshiaki Fuse*[a]

[a] *Department of Radiation Therapy, Japanese Red Cross Society Kyoto Daiichi Hospital, 15-749 Hommachi, Higashiyama-ku, Kyoto-shi, Kyoto 605-0981, Japan*

[b] *Department of Medical Physics, Graduate School of Medical Sciences, Kindai University, 377-2 Ohnohigashi, Osakasayama-shi, Osaka 589-8511, Japan*

[c] *Department of Central Radiology, Kindai University Hospital, 377-2 Ohnohigashi, Osakasayama-shi, Osaka 589-8511, Japan*

ARTICLE INFO

Article history:
Received 6 June 2019
Received in revised form
24 June 2019
Accepted 21 September 2019
Available online 2 November 2019

Keywords:
External body contour extended technique
Volumetric-Modulated arc therapy
Head and neck cancer
Eclipse

ABSTRACT

Aim: This study compared volumetric-modulated arc therapy (VMAT) plans for head and neck cancers with and without an external body contour extended technique (EBCT).
Background: Dose calculation algorisms for VMAT have limitations in the buildup region.
Materials and methods: Three VMAT plans were enrolled, with one case having a metal artifact from an artificial tooth. The proper dose was calculated using Eclipse version 11.0. The body contours were extended 2 cm outward from the skin surface in three-dimensional space, and the dose was recalculated with an anisotropic analytical algorithm (AAA) and Acuros XB (AXB). Monitor units (MUs) were set, and the dose distributions in the planning target volume (PTV), clinical target volume, and organ at risk (OAR) and conformity index (CI) with and without an EBCT were compared. The influence of a metal artifact outside of the thermoplastic head mask was also compared.
Results: The coverage of PTV by the 95% dose line near the patient's skin was increased drastically by using an EBCT. Plan renormalization had a negligible impact on MUs and doses delivered to OARs. CI of PTV with a 6-MV photon beam was closer to 1 than that with a 10-MV photon beam when both AAA and AXB were used in all cases. Metal artifacts outside the head mask had no effect on dose distribution.
Conclusions: An EBCT is needed to estimate the proper dose at object volumes near the patient's skin and can improve the accuracy of the calculated dose at target volumes.

* *Corresponding author.*
E-mail addresses: y.tanaka0316@gmail.com (Y. Tanaka), hmon@med.kindai.ac.jp (H. Monzen), kenji_356@yahoo.co.jp (K. Matsumoto), s_inocchi0805@gmail.com (S. Inomata), 20fu10se136red@gmail.com (T. Fuse).
https://doi.org/10.1016/j.rpor.2019.09.003

1. Background

Despite improvements in dose calculation algorithms implemented in radiotherapy treatment planning systems (TPSs) for calculation dose accuracy in regions of homo- and heterogeneity, the limitations in the buildup region have remained, and many investigators have tried to solve them.[1–10] Court et al.[4] reported that the agreement between the skin doses calculated by the pencil beam convolution (PBC) algorithm in the Eclipse™ TPS (Varian Medical systems, Palo Alto, CA, USA) and measured by the metal oxide semiconductor field effect transistor dosimeters was within ±20%. Oinam and Singh[6] evaluated the accuracy of the anisotropic analytical algorithm (AAA) in the Eclipse TPS version 8.6 for dose calculation in the buildup region by comparing the calculated doses with corresponding doses measured using the thermoluminescent dosimeter (TLD). AAA-calculated doses were lower by 7.56% than the TLD-measured doses at 0.2-cm depth. Rijken et al.[10] compared the surface doses measured with a radiochromic film (RCF) and calculated by the Pinnacle³® 9.10 (Koninklijke Philips N.V., Amsterdam, the Netherlands) using a thorax phantom immobilized by a vac bag and reported that measured surface doses were as much as double those calculated by the TPS. We face many problematic cases in clinical sites suspected to be near skin in intensity-modulated radiation therapy (IMRT) and volumetric-modulated arc therapy (VMAT) for head and neck cancers. In these cases, the dose prescribed to the primary or nodal target volume would not be estimated adequately, as several researchers have reported that model-based dose calculation algorithms generally underestimate the doses administered to surface and buildup regions.[4,6] Furthermore, acute skin toxicity caused by IMRT for head and neck cancers, such as radiation dermatitis, erythema, desquamation, and necrosis, has been a significant concern for radiation oncologists.[2,8,11,12] It is necessary to develop a technique that can calculate proper doses to the surface and buildup regions with commercial TPSs.

A simple technique to improve the calculated skin dose accuracy in a TPS was reported by Wang et al. as a feasibility study.[13] They showed that the performance of skin dose calculation with AAA by the Eclipse TPS improves when the body contour is extended by 1–2 cm outside the skin: the patient's skin dose predicted by Eclipse was brought within 4% of the MC-calculated dose by using this simple technique. The technique enables us to estimate the dose delivered to object volumes near the skin surface properly in VMAT for head and neck cancers, but the clinical impact of this has not been researched in past studies. They only investigated the dose prescribed to the skin and the primary or nodal target volumes located deep below the skin with a simple technique for real patient clinical treatment plans in their previous report.

2. Aim

In this study, to address the effectiveness of an external body contour extended technique (EBCT), we first compared the surface and isocenter doses administered to a phantom calculated by AAA and AXB with and without an EBCT, as measured by RCF and an ionization chamber. Then, VMAT plans for head and neck cancers with and without an EBCT were compared. The dose distributions to the planning target volume (PTV), clinical target volume (CTV), and organ at risk (OAR) and the conformity index (CI) with and without an EBCT were compared by using AAA and AXB not investigated in the previous study[13] in Eclipse TPS version 11.0. The influence of a metal artifact outside a thermoplastic head mask was also compared.

3. Material and methods

3.1. *Commercial TPS and dose calculation algorithms*

A commercial TPS (Eclipse version 11.0) was employed in this study. The dose calculation algorithms were AAA and AXB with heterogeneity correction. The photon energies were 6 and 10 MV, with flattened beams generated by a Novalis-Tx™ linear accelerator (Varian Medical systems and BrainLAB A.G., Heimstetten, Germany). The calculation grid size was 2.5 mm.[13] The dose reporting mode for AXB was set as dose-to-medium. The material table version 11.0 was used, and the material mapping was done automatically.

3.2. *Phantom study: comparison of the calculated and measured doses in the surface and isocenter regions*

To prepare for the basic experiments, Gafchromic EBT3 film (Lot No. 11151703; International Specialty Products, Wayne, NJ, USA) and a 0.6 cm^3 farmer chamber (TN30013; PTW, Freiburg, Germany) were used to measure the doses at the surface and isocenter of an I'mRT Phantom of size $18 \times 18 \times 18\ cm^3$ (IBA Dosimetry GmbH, Schwarzenbruck, Germany). Fig. 1 (a) shows the measurement of the surface dose using a thermoplastic head mask (CIVCO Medical Solutions, Kalona, IA, USA) with thickness of 2.4 mm and an EBT3 film cut to approximately $12 \times 12\ cm^2$ and placed at the central axis on the proximal phantom surface and sandwiched between the head mask and the I'mRT Phantom. A 0.6-cm^3 farmer chamber was inserted into the center of the I'mRT Phantom to measure the dose at the isocenter. Photon beams with energies of 6 and 10 MV from a Novalis-Tx linear accelerator were delivered at a gantry angle of 0° with a field size of $10 \times 10\ cm^2$, 200 MUs, and 100-cm source–detector distance (SDD).

We analyzed the EBT3 film doses according to previous reports.[14,15] An Epson Offirio ES-10000 G (Epson Seiko Corporation, Nagano, Japan) document scanner and FILM SCAN version 10.3.2 software were used to scan the irradiated films. The analysis software was the DD-system (DD-Analysis version 10.3.1; R-tech, Tokyo, Japan).

Computed tomography (CT) images of an I'mRT Phantom set inside a thermoplastic head mask, an EBT3 film, and a 0.6-cm^3 farmer chamber were imported into the Eclipse TPS. The external body contour was constructed manually to surround the contour of the I'mRT Phantom correctly because thermoplastic head masks are not included with it in the clinical

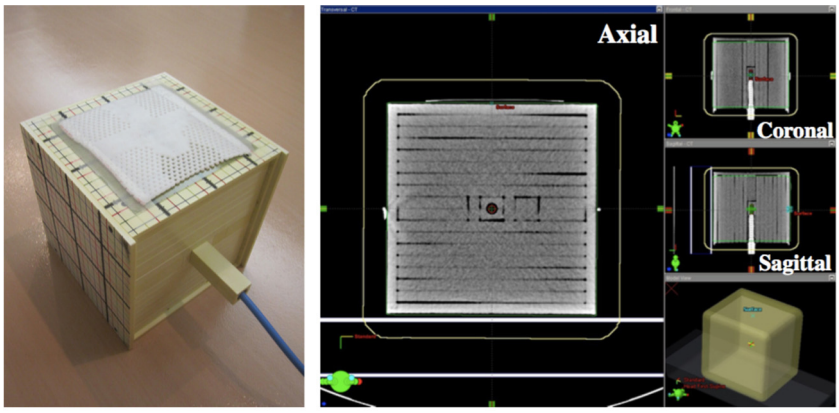

Fig. 1 – (a) Photograph and (b) axial, sagittal, and coronal CT images of an I'mRT Phantom set inside a thermoplastic head mask, EBT3 film, and 0.6-cm^3 farmer chamber. The CT images contain contoured structures for a 0.6-cm^3 farmer chamber, default body contour, and extended body contour represented by red, green, and yellow lines, respectively.

case. A structure representing the sensitivity area of a 0.6-cm^3 farmer chamber was also created to calculate the mean doses, as shown in Fig. 1 (b). We calculated the surface on which the EBT3 film was placed and the dose at the isocenter as point and mean doses using AAA and AXB with and without an EBCT under the same irradiation conditions as those under which the measurements were obtained. As part of the EBCT plans, the body contours were placed 2 cm outside the skin in three-dimensional space by use of the margin tool [Fig. 1 (yellow lines)]. For accurate comparison with the doses to the EBT3 films, the calculation grid size was set to 1.0 mm for the basic experiments.

3.3. *VMAT plans for head and neck cancers*

Three VMAT plans for head and neck cancers were investigated in this study. Clinical diseases had infiltrated near the skin in two cases, and one case had a metal artifact from an artificial tooth. Each patient characteristic was summarized in Table 1.

Each CT image was duplicated, and body contours were constructed using the body contour tool in Eclipse TPS with the threshold CT value set to −350 Hounsfield Units (HU). Gross tumor volumes (GTVs), CTVs, and OARs were copied from the practical treatment plans. For this study, to evaluate the dose in the buildup region adequately, we created the PTVs by extending the CTV 5 mm outward to the body contour.[16,17] Some cases were adjusted to satisfy the dose constraints for the OARs. The PTV was pulled back 2–3 mm from the skin only in the VMAT optimization to prevent boosting of the beamlets. The planning risk volume (PRV) margins were 3–5 mm for the spinal cord, brain, brainstem, and optic nerves. The CT value of soft or muscle tissue with a metal artifact was assigned as indicated by the relative electron density of water. Fig. 2 shows the axial CT images, including contoured structures, for all cases.

The prescribed dose was 70 Gy in 35 fractions, and the plan normalization mode was set so that 100% of the planned dose was administered to 95% of the PTV for all cases. The VMAT plans consisting of 2–3 full arcs were created with a 6-MV photon beam, and the doses were calculated with AAA in the Eclipse TPS. The Dose volume optimizer version 11.0 was set as the calculation model for the VMAT optimization. We refer to DXX% as the dose or percentage of the prescribed dose to XX% volume of the structural region in this study, and all VMAT plans were designed to satisfy the dose constraints for PTV and OARs following: D98% > 93%, D95% = 100%, and D2% < 115% for PTV, maximum dose (D_{Max}) < 125% for all irradiated volumes, D_{Max} < 50 Gy for PRV of the spinal cord, D_{Max} < 50 Gy for PRV of Brain and Brainstem, mean dose (D_{Mean}) < 26 Gy for at least one side parotid gland, D_{Max} < 40 Gy for the Eye ball, and D_{Mean} < 6 Gy for the Lens.

3.4. *Comparison of dose distributions with and without an EBCT on CT images*

The proper dose was calculated using an EBCT in all cases. In the plans described above, the body contours were placed 2 cm outside the skin surface in three-dimensional space by use of the margin tool [Fig. 2 (yellow lines)], and the dose was recalculated using AAA and AXB in the Eclipse TPS. A couch top was not included in the body contour extension in this study because Wang et al.[13] reported that the dose difference between skin with and without a couch was roughly 1%. First, the same MUs were set, and the dose distributions of PTV and CTV with and without an EBCT were compared. The percentages of the PTV receiving at least 95% of the prescribed dose were calculated and analyzed. D99% for CTV and D98%, D95%, D50%, D10%, and D2% for PTV were evaluated. Then, the plan normalization mode was reset so that 100% of the planned dose was administered to 95% of the PTV in the plan with an EBCT, and the dose delivered to the OARs was evaluated. Finally, to assess the adequacy of the photon energy for target volumes close to the surface, the CI of the PTV with a 6-MV photon beam was compared with that with a 10-MV photon beam using an EBCT.

Table 1 – Summary of the patient and tumor characteristics.

Case No.	Diagnosis	Stage	Tumor volume (cm^3)*	Tumor site
1	Maxillary sinus cancer	III	56.37	Maxillary sinus
2	Hypopharyngeal cancer	IVa	60.20	Pyriform sinus
3	Oropharyngeal cancer	I	3.87	Palatine tonsil

* Values for primary and nodal gross tumor volume.

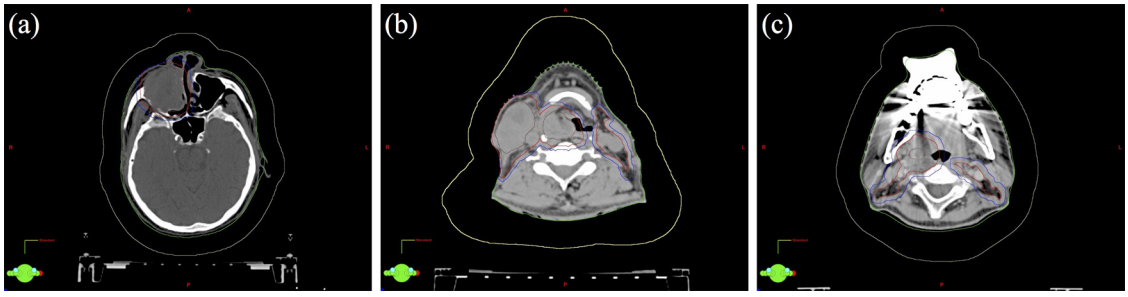

Fig. 2 – Axial CT images including contoured structures for all cases. Brown, red, blue, green, and yellow lines represent GTV, CTV, PTV, the default body contour, and the extended body contour, respectively. (a) The first case and (b) the second case have clinical diseases that extend near the skin, and (c) the third case has a metal artifact from an artificial tooth.

Table 2 – Surface and isocenter doses to an I'mRT Phantom for (a) 6- and (b) 10-MV photon beams measured by EBT3 film and a 0.6-cm^3 farmer chamber and calculated by AAA and AXB with and without an EBCT.

(a)

	Measurement	With an EBCT		Without an EBCT	
		AAA	AXB	AAA	AXB
Surface dose (Gy)	1.61	0.63	0.71	1.90	1.76
Isocenter dose (Gy)	1.58	1.61	1.61	1.59	1.60

(b)

	Measurement	With an EBCT		Without an EBCT	
		AAA	AXB	AAA	AXB
Surface dose (Gy)	1.16	0.61	0.56	1.60	1.42
Isocenter dose (Gy)	1.72	1.73	1.74	1.72	1.74

3.5. *Evaluation of the influence of a metal artifact outside the thermoplastic head mask*

In the case with a metal artifact, we also created the plan by assigning the CT value of the air layer outside the thermoplastic head mask influenced by the metal artifact to −1000 HU. The same MUs were set, and then dose recalculation was performed with AAA and AXB in the Eclipse TPS. The normalization value was reset, and the dose distributions of PTVs and OARs were compared with those without assignment of the CT value.

4. Results

4.1. *Results of phantom study: comparison of the calculated and measured doses in the surface and isocenter regions*

Table 2 indicates the doses to the surface and isocenter of an I'mRT Phantom measured by EBT3 films and a 0.6-cm^3 farmer chamber and calculated by AAA and AXB with and without an EBCT for 6- and 10-MV photon beams. For the 6-MV photon beam, although the difference of the surface dose between that measured by an EBT3 film and that calculated by AAA and AXB without an EBCT was −60.9% and −55.9%, respectively, an EBCT improved these results by 18.0% and 9.3%, respectively. About 2.0% of the difference in the isocenter dose between that measured by a 0.6-cm^3 farmer chamber and that calculated by both AAA and AXB without an EBCT was also ameliorated by 0.6% and 1.3% for AAA and AXB, respectively, by using an EBCT. The same tendency was observed in the results for the 10-MV photon beam.

4.2. *Results of comparison of the dose distributions of CT scanning with and without an EBCT*

Figs. 3 and 4 show the dose distributions calculated by AAA and AXB with and without an EBCT for two cases. The dose distributions described only by a 95% dose line are indicated in the lower row. The coverage of the PTV by the 95% dose line

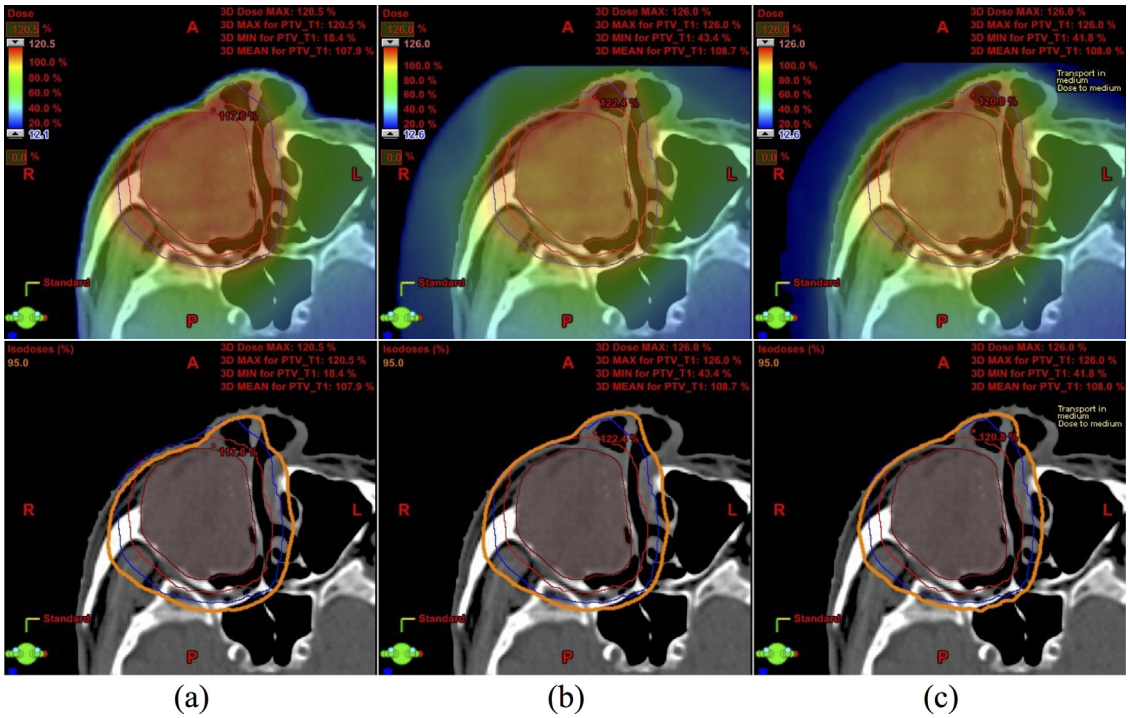

Fig. 3 – Contoured structures and dose distributions painted by a color wash (upper row) and the 95% dose line in orange (lower row) for the first case. The 6-MV VMAT plans with two full arcs calculated by (a) AAA without an EBCT, (b) AAA with an EBCT, and (c) AXB with an EBCT.

near the patient's skin was increased using an EBCT. Table 3 summarizes the percentage of the PTV receiving at least 95% of the prescribed dose (V95% for the PTV) for both cases. In the first case, although V95% for the PTV was only 95.8% with the default body contour, this increased to 99.4% and 98.8% for AAA and AXB with an EBCT, respectively. Similar results were obtained in another case. Fig. 5 illustrates the dose volume histograms (DVHs) of the PTV by using AAA and AXB with

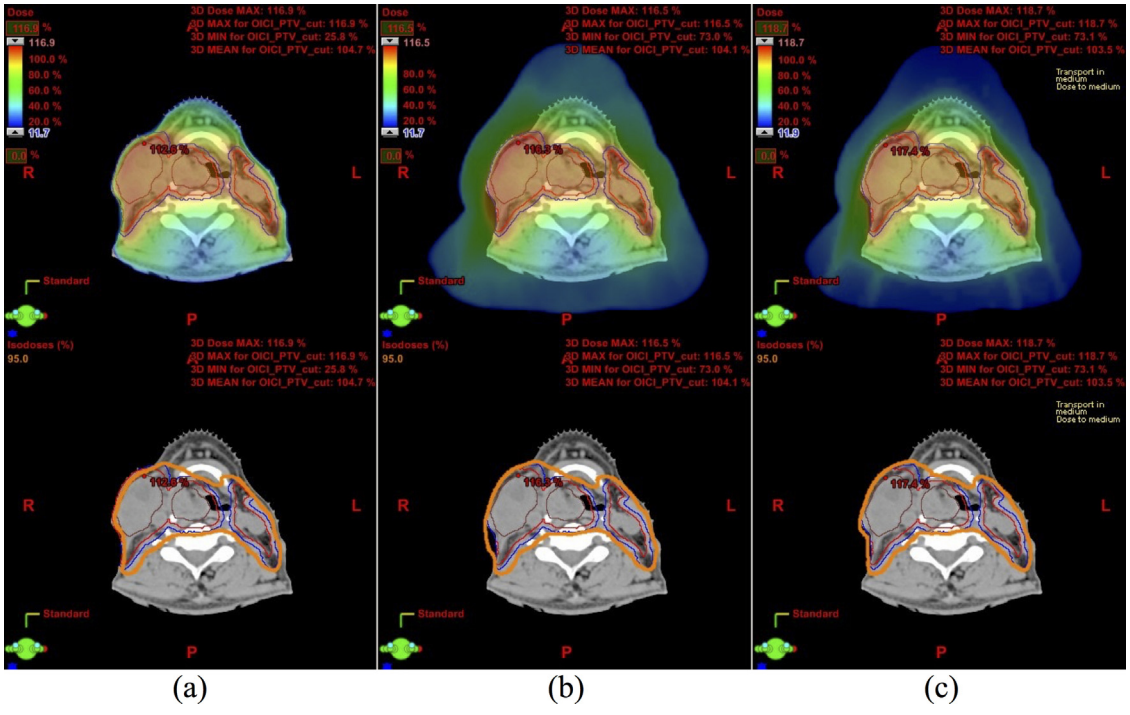

Fig. 4 – Contoured structures and dose distributions painted by the color wash (upper row) and the 95% dose line in orange (lower row) for the second case. The 6-MV VMAT plans with three full arcs calculated by (a) AAA without an EBCT, (b) AAA with an EBCT, and (c) AXB with an EBCT.

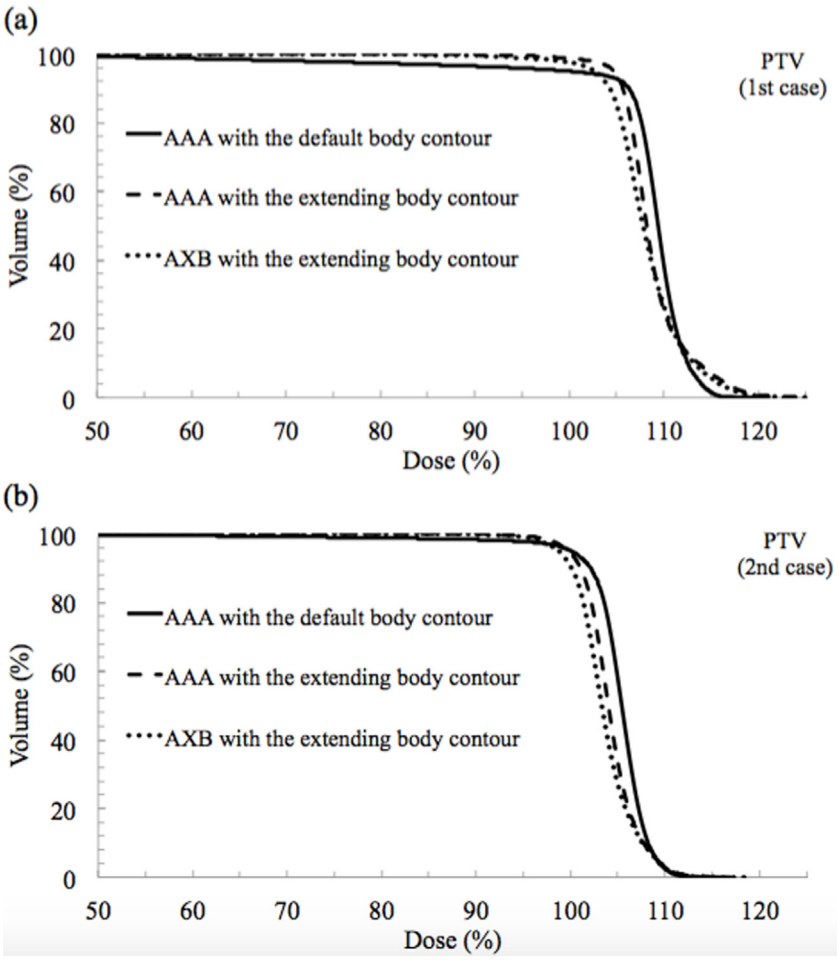

Fig. 5 – DVHs for the PTV obtained by AAA without an EBCT and AAA and AXB with an EBCT. PTVs from (a) the first case and (b) the second case.

Table 3 – Results of V95% for PTV calculated by AAA and AXB with and without an EBCT for the first and second cases.

	First case	Second case
	V95% for PTV (%)	V95% for PTV (%)
AAA without an EBCT	95.8	97.6
AAA with an EBCT	99.4	99.2
AXB with an EBCT	98.8	98.9

and without an EBCT for the first and second cases. An EBCT steepened the slope of the DVHs for both AAA and AXB. Table 4 lists the results of the dose-volumetric data for the PTV and CTV in two cases. In the first case, D99% for CTV and D98% for PTV were increased by up to 39.6% and 30.7%, respectively, by using an EBCT. Further, D99% for CTV and D98% for PTV were increased by 24.9% and 4.4%, respectively, for AAA with an EBCT in the second case. There was almost no difference in other dose-volumetric data from these two cases.

Table 5 summarizes the MUs and dose-volumetric data in the OARs after plan renormalization for the plans with an EBCT for the first and second cases. There was almost no difference in the MUs and dose-volumetric data in either case. However, the maximum dose to the right eyeball was 46.1 Gy

Table 4 – Results of the dose-volumetric data for the PTV and CTV calculated by AAA with and without an EBCT and AXB with an EBCT for (a) first and (b) second case.

(a)	AAA without an EBCT	AAA with an EBCT	AXB with an EBCT
CTV, D99% (%)	60.9	100.6	99.6
PTV, D98% (%)	71.5	102.2	98.7
PTV, D95% (%)	100.0	104.7	102.7
PTV, D50% (%)	109.4	108.1	107.8
PTV, D10% (%)	112.5	113.6	113.2
PTV, D2% (%)	114.7	118.0	117.3
(b)	AAA without an EBCT	AAA with an EBCT	AXB with an EBCT
CTV, D99% (%)	75.3	100.2	99.6
PTV, D98% (%)	93.4	97.8	96.8
PTV, D95% (%)	100.0	99.7	98.7
PTV, D50% (%)	105.4	104.0	103.3
PTV, D10% (%)	108.2	107.7	107.6
PTV, D2% (%)	110.2	110.6	110.4

Table 5 – MUs and dose-volumetric data for OARs after plan renormalization, calculated by AAA and AXB with and without an EBCT for (a) first and (b) second case.

(a)	AAA without an EBCT	AAA with an EBCT	AXB with an EBCT
MU	732	700	713
Eyeball (left), D_{Max} (Gy)	36.7	34.6	34.7
Eyeball (right), D_{Max} (Gy)	43.2	40.8	46.1
Lens (left), D_{Mean} (Gy)	9.2	8.8	8.9
Lens (right), D_{Mean} (Gy)	9.7	9.4	8.7
Optic nerve (left) (PRV), D_{Max} (Gy)	38.1	35.8	36.6
Optic nerve (right) (PRV), D_{Max} (Gy)	53.9	50.8	54.3
Brain (PRV), D_{Max} (Gy)	67.6	63.6	65.1
Brainstem (PRV), D_{Max} (Gy)	33.6	31.6	32.2
(b)	AAA without an EBCT	AAA with an EBCT	AXB with an EBCT
MU	790	793	801
Parotid gland (left), D_{Median} (Gy)	15.8	16.0	15.4
Parotid gland (right), D_{Median} (Gy)	15.6	15.8	15.3
Parotid gland (left), D_{Mean} (Gy)	24.0	24.1	23.7
Parotid gland (right), D_{Mean} (Gy)	26.7	26.7	26.4
Spinal cord (PRV), D_{Max} (Gy)	45.3	44.9	44.7
Brain (PRV), D_{Max} (Gy)	47.6	46.9	46.8
Brainstem (PRV), D_{Max} (Gy)	46.8	46.4	46.6

due to the dose increment near areas of low density, and this violated the general dose constraint for AXB.

In the first case, although the CI values of the PTV with a 6-MV photon beam were 1.11 and 1.09 for AAA and AXB without an EBCT, respectively, an EBCT improved these results by 1.01 and 1.03, respectively. The CI values of the PTV with a 10-MV photon beam were 1.09 and 1.11 for AAA and AXB with an EBCT, respectively, and were more distant to 1 than those obtained using a 6-MV photon beam for AAA and AXB with an EBCT. In the second case, although the CI value of the PTV with a 6-MV photon beam was 1.10 for both AAA and AXB without an EBCT, an EBCT improved these results by 1.09. The CI values of the PTV with a 10-MV photon beam was 1.10 for both AAA and AXB with an EBCT and were more distant to 1 than those obtained using a 6-MV photon beam for AAA and AXB with an EBCT.

4.3. *The influence of a metal artifact outside the thermoplastic head mask*

Fig. 6 shows the DVHs for the PTV and OARs calculated by AAA and AXB with and without assignment of the CT value of the air layer outside the thermoplastic head mask to −1000 HU for the third case (i.e., the one with the metal artifact). There was no difference between the dose distributions obtained using AAA and AXB.

5. Discussion

In this study, we investigated the clinical impacts on dose distribution of applying an EBCT to the clinical VMAT plan for head and neck cancers. Figs. 3–4 show that the VMAT plans with an EBCT for both AAA and AXB incorporated scattered radiation from an air layer and the thermoplastic head mask. Thereby, the coverage of the PTV by the 95% dose line near the patient's skin was drastically increased for all cases, and D99% for the CTV and D98% for the PTV were increased by up to 39.6% and 30.7%, respectively, in Table 4. Wang et al.[13] reported that AAA with the default body contour underestimated the skin dose by more than 14% of the prescription dose to avoid including patient immobilization devices in the calculation volume.[2] Their feasibility study showed that this underestimation could be improved by extending the body contour to encompass at least 1 cm of the air outside the skin by comparison with the MC-calculated dose validated using the optically stimulated luminescence dosimeters. The results posed a problem for clinical use, however, they did not describe clinical values because they only illustrated that the DVHs for the PTVs from the VMAT plan which the primary or nodal target volumes were located deep below the skin were not affected by using an EBCT. An EBCT could improve the accuracy of the calculated dose to the surface and buildup regions, especially for problematic cases in which clinical diseases infiltrate nearby skin and enable us to estimate the proper dose to the target volume. Proper estimation might reduce the dose delivered to OARs more than ever before and prevent radiation toxicity.[2,8,11,12] In future work, we will attempt to apply an EBCT to more clinical cases to further verify the clinical impact on dose distributions.

The doses at deeper target volumes or OARs are not affected by an EBCT.[13] Our results also showed that plan renormalization had a negligible impact on the MUs and doses delivered to OARs. However, re-optimization was not performed for any of the plans investigated in this study to evaluate clearly the impact of an EBCT on non-optimized calculations but the calculation dose accuracy in the VMAT plan for head and neck cancer whose object volumes are located near patient's skin, and the MUs and doses to OARs calculated by AAA and AXB with an EBCT might not have been evaluated sufficiently. Because the shape of the DVHs for the target volumes changed significantly, the clinical dose distribution might have impacted the volume normalization in the IMRT plan. Further, it is necessary to examine a suitable technique for the optimization in VMAT planning with an EBCT.[18,19]

An EBCT improved the CI values of the PTVs with a 6-MV photon beam; especially, those were improved by approximately 1 for both AAA and AXB in the first case. The reason for this was that the coverage of the PTV by the 95% dose line near the patient's skin was improved significantly by using an EBCT. Mynampati et al.[20] created the American Association of Physics in Medicine Task Group 119 benchmark plans[21] for the VMAT plan and showed that the CI of the head and neck test case was 1.09 with a 6-MV photon beam. Our results were equal to or better than theirs, and the dose conformity of the PTVs with a 6-MV photon beam had higher performance than that with a 10-MV photon beam. However, we also should

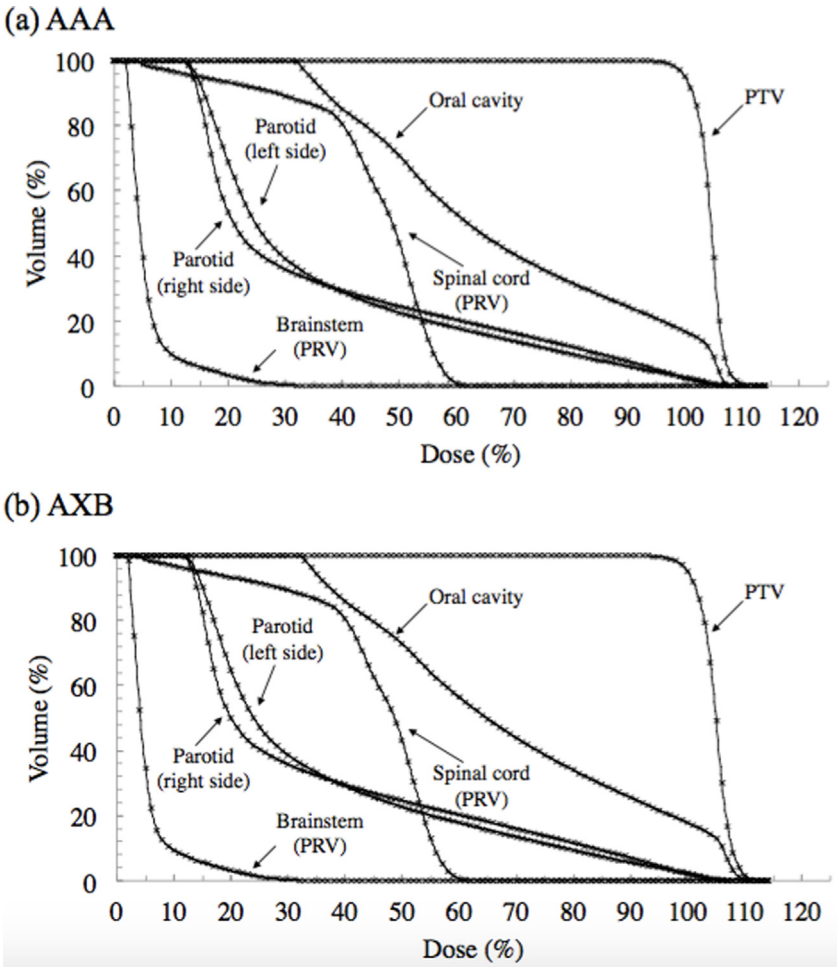

Fig. 6 – DVHs for PTV and OARs obtained by (a) AAA and (b) AXB with an EBCT in the third case. Solid lines and cross plots are DVHs with and without assignment of the CT value of the air layer outside the thermoplastic head mask with a metal artifact to −1000 HU.

evaluate the dose distributions in the VMAT plan with a 10-MV photon beam in the case of deep-seated head and neck cancers.

We verified the effects of an EBCT on the calculation of dose accuracy in the surface and buildup regions through our basic experiments (Table 2). An RCF might be suitable to measure the surface dose: Bilge et al. reported that the surface doses administered to an EBT film and a Markus parallel plate ionization chamber agreed within 5% for a 6-MV photon beam.[22] However, EBT3 measurement doses converted from dose-response curves with analog-to-digital converter values are relative doses that are regarded as an index of the surface dose.[23] Our results showed that an EBCT obviously improved the accuracy of dose calculation in the surface region by including a thermoplastic head mask in the body contour, but the dose difference was still large even if an EBCT was used. An RCF has several characteristics,[15,24,25,26] and Borca et al.[25] indicated that overall uncertainty of 1.7% was observed with an EBT3 film. Moreover, surface dose measurement is very challenging, and it has been investigated in several studies.[27–30] The measurement errors with commonly used detectors (including an RCF) while comparing the surface dose using the PTW 30–360 extrapolation chamber (PTW, Freiburg, Germany) ranged from −0.1% to 26% before any corrections were applied.[27] This is a limitation of this study; new, special dosimeter systems or correction factors for measurement of the doses in the surface and buildup regions might be necessary.

6. Conclusions

An EBCT that uses AAA and AXB as components of the VMAT plan for head and neck cancers is needed to estimate a proper dose at object volumes near patient skin and can improve the accuracy of dose calculation in the target volumes.

Conflict of interest

None declared.

Financial disclosure

None declared.

Acknowledgements

We thank Richard Lipkin, PhD, from Edanz Group (www.edanzediting.com/ac) for editing a draft of this manuscript.

REFERENCES

[1]. Chung H, Jin H, Dempsey JF, Liu C, Palta J, Suh TS, et al. Evaluation of surface and build-up region dose for intensity-modulated radiation therapy in head and neck cancer. *Med Phys* 2005;**32**:2682–9.
[2]. Hadley SW, Kelly R, Lam K. Effects of immobilization mask material on surface dose. *J Appl Clin Med Phys* 2005;**6**:2005.
[3]. Court LE, Tishler RB. Experimental evaluation of the impact of different head-and-neck intensity-modulated radiation therapy planning techniques on doses to the skin and shallow targets. *Int J Radiat Oncol Biol Phys* 2007;**69**:607–13.
[4]. Court LE, Tishler RB, Allen AM, Xiang H, Makrigiorgos M, Chin L. Experimental evaluation of the accuracy of skin dose calculation for a commercial treatment planning system. *J Appl Clin Med Phys* 2008;**9**:2008.
[5]. Panettieri V, Barsoum P, Westermark M, Brualla L, Lax I. AAA and PBC calculation accuracy in the surface build-up region in tangential beam treatments. Phantom and breast case study with the Monte Carlo code PENELOPE. *Radiother Oncol* 2009;**93**:94–101.
[6]. Oinam AS, Singh L. Verification of IMRT dose calculations using AAA and PBC algorithms in dose buildup regions. *J Appl Clin Med Phys* 2010;**11**:2010.
[7]. Kry SF, Smith SA, Weathers R, Stovall M. Skin dose during radiotherapy: a summary and general estimation technique. *J Appl Clin Med Phys* 2012;**13**:2012.
[8]. Lee N, Chuang C, Quivey JM, Phillips TL, Akazawa P, Verhey LJ, et al. Skin toxicity due to intensity-modulated radiotherapy for head-and-neck carcinoma. *Int J Radiat Oncol Biol Phys* 2002;**53**:630–7.
[9]. Joseph K, Rose B, Warkentin H, Yun J, Ghosh S, Tankel K. Peri-anal surface dose in anal canal VMAT radiotherapy. *J Med Imaging Radiat Oncol* 2018;**62**:734–8.
[10]. Rijken J, Kairn T, Crowe S, Muñoz L, Trapp J. A simple method to account for skin dose enhancement during treatment planning of VMAT treatments of patients in contract with immobilization equipment. *J Appl Clin Med Phys* 2018;**19**:239–45.
[11]. Hoppe BS, Laser B, Kowalski AV, Fontenla SC, Pena-Greenberg E, Yorke ED, et al. Acute skin toxicity following stereotactic body radiation therapy for stage 1 non-small-cell lung cancer: who's at risk? *Int J Radiat Oncol Biol Phys* 2008;**72**:1283–6.
[12]. Radaideh KM, Matalqah LM. Predictors of radiation-induced skin toxicity in nasopharyngeal cancer patients treated by intensity-modulated radiation therapy: a prospective study. *J Radiother Pract* 2016;**15**:276–82.
[13]. Wang L, Cmelak AJ, Ding GX. A simple technique to improve calculated skin dose accuracy in a commercial treatment planning system. *J Appl Clin Med Phys* 2018;**19**:191–7.
[14]. Nakayama S, Monzen H, Oonishi Y, Mizote R, Iramina H, Kaneshige S. A novel method for dose distribution registration using fiducial marks made by a megavoltage beam in film dosimetry for intensity-modulated radiation therapy quality assurance. *Phys Med* 2015;**31**:414–9.
[15]. Kamomae T, Oita M, Hayashi N, Sasaki M, Aoyama H, Oguchi H, et al. Characterization of stochastic noise and post-irradiation density growth for reflective-type radiochromic film in therapeutic photon beam dosimetry. *Phys Med* 2016;**32**:1314–20.
[16]. Dionisi F, Palazzi MF, Bracco F, Brambilla MG, Carbonini C, Asnaghi DD, et al. Set-up errors and planning target volume margins in head and neck cancer radiotherapy: a clinical study of image guidance with on-line cone-beam computed tomography. *Int J Clin Oncol* 2013;**18**:418–27.
[17]. Delishaj D, Ursino S, Pasqualetti F, Matteucci F, Cristaudo A, Soatti CP, et al. Set-up errors in head and neck cancer treated with IMRT technique assessed by cone-beam computed tomography: a feasible protocol. *Radiat Oncol J* 2018;**36**:54–6.
[18]. Nguyen TB, Hoole AC, Burnet NG, Thomas SJ. The optimization of intensity modulated radiotherapy in cases where the planning target volume extends into the build-up region. *Phys Med Biol* 2009;**54**:2511–25.
[19]. Ashburner MJ, Tudor S. The optimization of superficial planning target volumes (PTVs) with helical tomotherapy. *J Appl Clin Med Phys* 2014;**15**:2014.
[20]. Mynampati DK, Yaparpalvi R, Hong L, Kuo HC, Mah D. Application of AAPM TG 119 to volumetric arc therapy (VMAT). *J Appl Clin Med Phys* 2012;**13**:2012.
[21]. Ezzell GA, Burmeister JW, Dogan N, LoSasso TJ, Mechalakos JG, Mihailidis D, et al. IMRT commissioning: multiple institution planning and dosimetry comparisons, a report from AAPM Task Group 119. *Med Phys* 2009;**36**:5359–79.
[22]. Bilge H, Cakir A, Okutan M, Acar H. Surface dose measurements with GafChromic EBT film for 6 and 18 MV photon beams. *Phys Med* 2009;**25**:101–4.
[23]. Sankar A, Ayyangar KM, Nehru RM, Kurup PG, Murali V, Enke CA, et al. Comparison of Kodak EDR2 and Gafchromic EBT film for intensity-modulated radiation therapy dose distribution verification. *Med Dosim* 2006;**31**:273–82.
[24]. Niroomand-Rad A, Blackwell CR, Coursey BM, Gall KP, Galvin JM, McLaughlin WL, et al. Radiochromic film dosimetry: recommendations of AAPM radiation therapy committee task group 55. American association of physicists in medicine. *Med Phys* 1998;**25**:2093–115.
[25]. Borca VC, Pasquino M, Russo G, Grosso P, Cante D, Sciacero P, et al. Dosimetric characterization and use of GAFCHROMIC EBT3 film for IMRT dose verification. *J Appl Clin Med Phys* 2013;**14**:4111.
[26]. Devic S, Tomic N, Lewis D. Reference radiochromic film dosimetry: Review of technical aspects. *Phys Med* 2016;**32**:541–56.
[27]. Reynolds TA, Higgins P. Surface dose measurements with commonly used detectors: a consistent thickness correction method. *J Appl Clin Med Phys* 2015;**16**:358–66.
[28]. Akbas U, Kesen ND, Koksal C, Bilge H. Surface and buildup region dose measurements with Markus parallel-plate ionization chamber, Gafchromic EBT3 film, and MOSFET detector for high-energy photon beams. *Adv. High Energy Phys* 2016;**2016**:8361028.
[29]. Sigamani A, Nambiraj A, Yadav G, Giribabu A, Srinivasan K, Gurusamy V, et al. Surface dose measurements and comparison of unflattened and flattened photon beams. *J Med Phys* 2016;**41**:85–91.
[30]. Akbas U, Kesen ND, Koksal C, Okutan M, Demir B, Becerir HB. Surface dose measurement with Gafchromic EBT3 film for intensity modulated radiotherapy technique. *EPJ Web Conf* 2017;**154** (2017)01011.